Contents

List of Figures

List of Tables

Chapter 1

Introduction

> "Every competent physicist can "do" quantum mechanics, but the stories we tell ourselves about what we are doing are as various as the tales of Sheherazade, and almost as implausible."
>
> David J. Griffiths

The International System of Units (SI, abbreviated from the French Système international d'unités) emerged in the late 18^{th} century as a coherent metric system of measurement with rationally related units and simple rules for combining them [**?**]. Since its inception it was improved and augmented continously in an ongoing effort to accomodate continuued scientific and technological progress. The current SI system is comprised of seven base units: The kilogram (kg), the second (s), the Ampere (A), the Kelvin (K), the mole (mol) and the candela (cd). Currently a redefinition of four of base units (kilogram, mole, Kelvin, Ampere) in terms of fundamental constants is under way [**?**, **?**, **?**]. The proposed change will improve the definitions of these base units to make them easier to realize experiemntally, particularily for the measurement of electrical quantities [**?**]. It will also eliminate the last remaining base unit definition which relies on a historic material artefact, the international prototype of the kilogram. As a result all base units will, for the first time, be tied to one or more fundamental constants of nature.

As these developments are put into motion, similar discussions regarding the SI base unit for luminous intensity, the candela, have emerged. It has been suggested that it can be improved by leveraging recent advances in classical radiometry and photometry as well as the development of novel quantum devices and techniques [**?**].

At the time of writing the definition of the candela read:

> The candela is the luminous intensity, in a given direction, of a source that emits monochromatic radiation of frequency $540 \times 10^{12}\,\mathrm{Hz}$ and that has a radiant intensity in that direction of $638^{-1}\mathrm{W\,sr^{-1}}$.

Traditional applications relying on this definition in conjunction with accurate photometric and radiometric measurements are light design, manufacturing and use of optical sources, detectors, optical components, colored materials and optical radiation measuring equipment [**?**]. In the classical regime of optical radiation high flux levels dominate. Here primary optical radiation scales for sources and detectors are generally based on cryogenic radiometry estab-

lishing a link to the SI units of electricity [?]. Other calculabe sources such as synchrotrons and blackbody radiators can serve as primary source scales in the ultraviolet and deep-UV regions by establishing tracability to SI units of thermometry, electricty and length [?, ?].

Scaling down to the quantum world of radiometry is associated with a loss of measurment accuracy. In this regime dedicated photon counting techniques are required to deal with the challenge of low flux levels. Since they rely on counting photons directly, the can provide efficient and traceable measurements and improved uncertainties. For high-accuracy absolute radiometry in this regime predictable single or quasi-single-photon sources and photon detectors as well as associated new quantum-based callibration methods and standards are called for. To promote the development of such technologies a reformulation of the candela has been proposed in terms of *countable* photon units [?, ?, ?, ?, ?]. Here we emphasize the distinction between *countable* and *calculabe* sources of photons. The latter being available as blackbodies or synchrotron radiators.

A straightforward quantum-based reformulation has been suggested based on [?, ?]:

$$P = nh\nu, \tag{1.1}$$

where the radiant intensity per steradian $P = 638^{-1}\,\mathrm{W\,sr^{-1}}$ in a given direction and the photon frequency $\nu = 540 \times 10^{12}\,\mathrm{Hz}$ are assumed to be exact with their numerical values inherited from the present definition of the candela. The anticipated proposed changes to the SI system will define Planck's constant $h = 6.626\,070\,15 \times 10^{-34}\,\mathrm{J\,s}$ as an exact numerical constant [?]. As a consequence the number of photons per second per steradian in a candela n becomes a constant defined as:

$$n = \frac{P}{h\nu} \approx 4.091\,942\,9 \times 10^{15}\,\mathrm{counts\,s^{-1}\,sr^{-1}}. \tag{1.2}$$

Given this definition of the radiant intensity of a candela in terms of countable photons, a possible formulation of the quantum candela could read:

> The candela is the luminous intensity, in a given direction, of a source that emits photons of frequency $540 \times 10^{12}\,\mathrm{Hz}$ at a rate of $4.091\,942\,9 \times 10^{15}$ photons per second per steradian in that direction.

This definition would incur a change of 0.0014 % from the current value of the candela, an acceptable change, taking into account the fact that current experimental realizations of the candela are limited to uncertainties of 0.02 % [?]. Proposals such as this are regularly reviewed by the Consultative Committee for Photometry and Radiometry ensuring that the current best measurement practices and existing as well as emerging needs of the user community of the candela are met [?].

While a proposed formulation of a quantum-candela can be considered a small change to the SI system, a shift towards quantum based radiometic SI units it likely to become a critical enabler driving the development of accurate and traceable measuerment methods on the single-photon level. In order for the definition of the quantum-candela to have practical meaning, photon counting detectors are required. To ensure proper calibration of such devices, reliable deterministic single photon sources are required. As novel instruments and associated calibartion standards emerge, our ability to work with individual photons in a wide range of

applications will improve [?, ?, ?, ?]. The quest for single photon sources is supported by large research projects such as “Single-Photon Sources for Quantum Technology" funded by European Metrology Research Program.

Advances in radiometry are particularily important for fields like quantum communication and quantum computing. They are heavily reliant on deterministic reliable single-photon sources and well-calibrated detectors capable of resolving single photons. As such they have acted as major driving forces in their development [?, ?]. Amongst others, some well known applications include quantum key distribution [?, ?, ?] or transmission in a quantum network [?, ?, ?].

At present several candidates for on-demand single-photon sources are available: One consists of a laser beam attenuated such that the mean number of photons in the beam becomes close to one [?, ?, ?]. However, the mean photon number cannot be controlled perfectly and a non-zero probability remains that multiple photons are present.

Quasi-single photon states can be realized more efficiently using photon-pairs, consisting of a signal and an idler photon. Pairs are created when a photon interacts with a non-linear optical medium in a process called spontaneous parametric down-conversion (SPDC) [?, ?, ?, ?, ?, ?]. The deciding feature of the process is the strong time-correlation between the signal and idler photons. If both photons are injected into individual signal paths, an detection event in one of the paths heralds the existence of a photon in the other path. SPDC pairs can thus be used to construct single-photon sources. Unfortunately, due to the poor efficiency of the SPDC process, the probability of generating pairs is unfavorable [?, ?]. Thus efforts have been undertaken to improve the effeciency [?, ?, ?].

Quantum dots emit photons by recombination of electron-hole pairs created by optical excitation or via an electric current [?, ?, ?]. The choice of semiconducting material determines the electronic structure of the system and thus the characteristics of the emitter. Similarily single-photons can be obtained as a result of radiative transitions between energy levels of single atoms or molecules trapped in an optical cavity [?]. While these sources have desirable properties such as high-collection efficiency, the practical usefulness is limited due to their technilogical requirements, amongst others a high vaccuum is needed to operate these sources [?].

For a wide range of single photon sources, significant progress has been made towards improving purity, indistinguishability and collection efficiency [?, ?, ?, ?, ?].

However, a single photon source suitable for the calibration of single-photon detectors is difficult to realize [?]. Ideally, a standard single photon source should be emmitting with a quantum efficiency of 100 % indicating that the entire exitation energy is transformed into radiation without losses. At the same time single photons should be emitted with a probability of one and subsequently collected with perfect efficiency.

Very recently, steps towards realizing an ideal deterministic single photon source have been taken. In particular it has been demonstrated that color centers in nanodiamonds involving silicon [?, ?] and nitrogen [?] are promising candidates for the realization of standard single photon sources [?, ?]. Single photon sources were absolutely calibrated by a classical detector and a calibrated spectormeter. Thus a unbroken traceability chain to the SI system has been achieved. The photon flux of the source can be controlled via the settings of the pump laser repetition rate. In this way a direct link between the high photon flux levels of the classical

regime and low photon flux levels in the quantum world has been established. For the nitrogen vacancy center a photon flux rate of $\approx 1.4 \times 10^5$ photons per second was established.

In this thesis we focus on the silicon-vacancy center hosted in nanodiamond and its properties as a single photon source. In doing so we aim to add momentum to the application of single photon source as high accuracy calibration devices and subsequently, to the development of photon counting detectors and the adoption of the quantum-candela.

The SiV center in diamond is an ideal candidate for single photon calibration purposes. It is are very efficient and stable narrow linewidth emitter, emitting single photons with high intensity. Conveniently, SiV centers operate at room temperature under normal pressure and hence do not require extremely sophisticated experimental setups. As an alternative to hosting SiV centers in bulk diamond, they can be implanted in nano-sized diamond grains offering increased collection efficiency. Grains containing individual SiV centers can be indentified and preselected according to their properties. As a result individual emmitters can be made mobile using pick-and-place techniques. The ability to relocate emitters is convenient since it unlocks applications requiring selected single emitters such as coupling to antennas or the use as hybrid integraded single photon sources in conjunction with vertical-cavity surface-emitting laser (VCLS).

In this thesis we synthesize nanodiamonds with SiV centers using a variety of different techniques. Chemical vapor deposition, high-pressure, high-temperature synthesis as well as wet-milling methods are used to produce a sizeable set of samples. To investigate the samples, i.e to study the optical properties of embedded SiV centers we rely on optical excitation. In particular, confocal microscopy is used to collect emitted flourescent single-photons. An attached spectrometer or a Hanbury Brown and Twiss setup offer further insights into the properties of the SiV center as a single photon source. We examine a large number of individual SiV centers produced with different methods, allowing us to establish distributions of selected SiV center properties. To our knowledge, this is the largest coherent examination of this type to date. After charting the luminescence properties of emmitters, we examine the possibilities of coupling SiV centers to antennas and study the effect. Furthermore, we explore the use of SiV centers in combination with a VCLS.

The thesis is structured as follows: chapter 2 introduces the reader to color centers and diamond as a host material. A detailed discussion of SiV centers and their most important luminous properties is presented. **??** familiarizes the reader with the essential experimental setup and methods depolyed in this thesis to study SiV centers. Various relevant methods of synthesizing SiV centers in nanodiamonds are presented and discussed in **??**. **??** is dedicated to the important topic of gauging the quality of the fabricated samples. The results of investigating the luminous properties of our SiV center samples is presented in **??**. The possibility of coupling single SiV centers to photonic structures is investigated in **??**. Finally we summarize and discuss our findings of this thesis in **??**.

Chapter 2

Silicon Vacancy Centers in Diamond

In the following we introduce color centers, i.e. optically acive point-defects, present in a diamond lattice. We focus on color centers combining silicon impurties and lattice vacancies (SiV) in particular since their experimental study is at the focus of this thesis. We start by presenting the most important properties of diamond and emphasize its suitability as a host for optical applications with color centers. A classification of diamond with respects to defects and impurities as well as crystallinities serves as a preparation for the introduction of methods to synthetize diamonds containing SiV centers presented in **??**. Finally, we discuss SiV centers in detail and focus on their most important optical properties as reliable single-photon sources at room temperature. In particular, we zoom in on the key features of its luminescence spectrum, the zero-phonon-line and the phonon side band. Our discussion partially follows the presentation in [**?**, **?**, **?**, **?**].

2.1 Diamond as a host lattice

Diamond is a metastable modification of carbon which is, in fact, stable under normal pressure and at room temperature [**?**]. Carbon atoms form strong $sp3$-bonds with each other in a tetraedal arrangement of neighboring atoms. The resulting $sp3$-hybridized lattice is of exceptional mechanical stability, making diamond the hardest known material [**?**]. The crystal structure can also be interpreted as a face-centered cubic (fcc) lattice with two carbon atoms in the primitive Bravais cell, situated at $(0, 0, 0)\ a$ and $(\frac{1}{4}, \frac{1}{4}, \frac{1}{4})\ a$ with $a = 3.567\,\text{Å}$ denoting the lattice constant [**?**]. Figure 2.1 illustrates the structure.

The valence and conduction bands of diamond are separated energetically by a large direct band gap of 7.3 eV while its indirect band gap amounts to 5.5 eV [**?**, **?**]. As a result diamonds are transparent for light of all wavelengths larger than 230 nm [**?**]. This transparent quality makes diamond an ideal host material for various optically active lattice defects or impurities. These induce a wide range of discrete energy levels accomodated by the sizable band gap. The absorption of optically active impurities or impurity complexes gives rise to the color of diamonds, thus these impurities are commonly termed color centers [**?**]. Due to the exceptional mechanical stability of diamond color centers too are very stable, another important property enabling optical applications.

A property of diamond, detremental to some optical applications, is its large refractive index

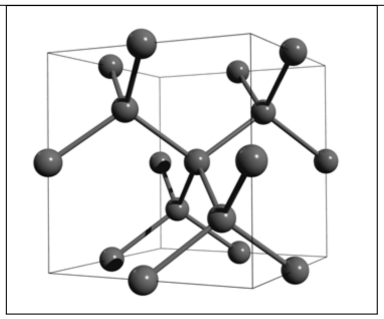

Figure 2.1: Face-centered cubic diamond lattice. Note the tetraedal arrangements of carbon atoms. Figure reproduced with permission from [**?**].

with values of 2.49 at 360 nm and 2.4 at 800 nm respectively [**?**]. Thus, a portion of the flourescent light escaping from the diamond is reflected back into it, effectively reducing the efficiency of light extraction. If nanodiamonds smaller than the wavelenght of the light to be collected are used, internal reflection is supressed and the extraction efficiency can be increased [**?**].

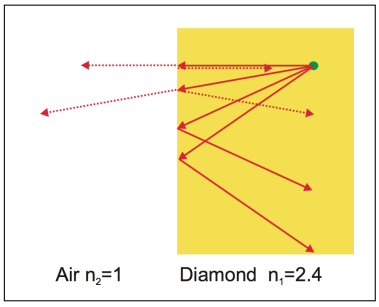

Figure 2.2: Light from a flourescent emmitter inside the diamond (green dot) undergoes reflection at the diamond-air interface. Figure reproduced with permission from [**?**].

2.2 Classification of diamond

Two major approches for classifying diamond are commonly encountered. First, classification according to the presence or absence of certain impurities or impurity complexes. Second, classification based on different diamond crystallinities observed. In the following both classification systems are briefly introduced.

2.2.1 Classification by impurities

Impurities or complexes of impurities in the diamond lattice can be optically active and thus change the optical properties of diamond. Most strikingly perhaps is the appearence of color in otherwise colorless diamond due to a sufficient concentration of such defects. Using IR absorption spectroscopy the degree of nitrogen impurtities can be determined. It is used to subdivide diamonds into distinct groups named Type I and Type II [**?**, **?**]. The groups are further subdivided as follows:

- Type Ia: With a nitrogen concentration of up to 3000 ppm most natural occuring diamonds belong to this group [**?**]. Nitrogen appears arranged predominantly in aggregate clusters forming complexes of impurties. These complexes are optically active, absorbing light in the blue range of the visible spectrum. Consequently Type Ia diamonds often exhibit a yellow to brownish coloration.
- Type Ib: With concentrations of up to 500 ppm nitrogen atoms appear predominantly in isolation, replacing individual carbon atoms in the diamond lattice. In addition to absorbing visible blue light, green is being absorbed as well. Type Ib diamond thus exibits intensified the yellow or brownish coloration. While only 0.1 % of naturally occuring diamond fall into this class, almost all synthetic diamonds created using the high-pressure, high-temperature (HPHT) method are of Type Ib [**?**].

While Type I diamond exhibits an appreciable concentration of nitrogen, Type II diamonds lack nitrogen entirely. Type II diamond is divided into two subgroups according to the presence or absence of boron as follows:

- Type IIa: Can be considered pure as they lack boron impurities and other optically active defects [**?**]. They thus are colorless. Up to 2 % of natrually occuring diamond and most diamonds synthetically created using the chemical vapor deposition (CVD) method are of Type IIa [**?**].
- Type IIb: Contains appreciable concentrations of boron atoms replacing individual carbon atoms in the diamond lattice. Boron defects are optically active absorbing visible light ranging from red to yellow. Depending on the Boron concentration blue to grey colorations are observed. Furthermore, diamond is turned from an insulator to a efficient p-type semiconductor in the presence of boron impurities [**?**].

We remark that for many modern applications of diamonds the presented “classic" categorisation of diamond is not enough. In these cases a precise quantification of the concentration and nature of various relevant impurities is called for [**?**, **?**].

In this section we also briefly touched upon the CVD and HPHT methods, two approaches to synthetically produce diamonds. Both are relevant for this thesis and are explained in detail in **??**.

2.2.2 Classification by crystallinity

Up unitl now, the discussion assumed that diamond forms a lattice consisting of one giant single crystal. However, other crystallinities are possible and can be used to classify diamond. They range from mono or single crystals to polycrystalline, nanocrystalline or even ultra-nanocrystalline diamond films [**?**]. This classification is particularirly useful for synthesized diamon as will be discussed in **??**. Table 2.1 summarizes the different sizes of diamonds or diamond films which can be achieved using variations of the CVD method.

Diamond films consist of isolated diamond grain of random orientation with sp2 hybridized grain boundaries and graphit-like inclusions [**?**]. Carbon present in non-diamond phases, e.g. graphite or amorphous carbon gives rise to detremental light absorption while crystal boundaries lead to increased scattering losses. As the size of diamond crystallites get smaller, the

ratio of non-diamond carbon to diamond carbon increases. Thus losses are most pronounced for the smallest grain diamond films.

Table 2.1: Classification of diamonds sythensized using CVD [?].

Crystallity	Grain size
monocrystalline	arbitrary
polycrystalline	50 nm to 10 µm
nanocrystalline	10 nm to 50 nm
ultra-nanocrystalline	< 10 nm

2.3 Silicon-vacancy center

A color center is an optically active point-defect in a crystall lattice, capable of absorbing and emitting light. Defects can consist of one or several vacant lattice sites, foreign atoms replacing lattice atoms or a combination thereof. If the precence of a defect induces discrete energy levels located in the band gap of the host material, the color center can be interpreted as its own quantum system. In other words, the color center can be viewed as a single isolated and localized artificial atom embedded in a host matrix. As such it is able to absorb light and emit single photons by means of flouresence.

Compared to alternative single photon sources like single atoms [?], Ions [?] or individual quantum dots [?, ?], color centers offer a couple of advantages due to their solid state environment. As a result of the high mechanical stability of the host lattice color centers exhibit increased photo-stability, in particlar compared to organic molecules as light sources. Furthermore the host lattices offers protection for color centers from detremental interactions with agressive free molecules [?]. Lastly, color centers can be handled and investigated at room temperature, thus significantly reducing the experimentall efforts necessary to study them.

Of particular interest are color centers as single photon sources when hosted in diamond. With its transparency, exceptional stability and minimal phononic interactions at room temperature the diamond lattice is an ideal host matrix for color centers [?, ?]. While more than 500 different color centers in diamond are documented, only a small fraction has been investigated with respect to their properties as single photon sources [?]. For an in-depth review of color centers and their versatile applications see [?, ?]. The two arguably most prominent examples of well-studied color centers are vacancy centers featuring nitrogen and silicon [?, ?, ?].

The silicon-vacancy (SiV) center in diamond and its properties is at the center of this thesis. The SiV center has been established as an efficient single photon source at room temperature. It shows very narrow emmisiion lines with record count rates up to 6.2×10^6 cps (counts-per-second) [?]. The emmision of indistinguishable photons and the optical access of electronic spin states have been demonstrated [?, ?, ?, ?], hinting at the possibility of deploying SiV centers as spin-qubits.

A silicon-vacancy center is formed in a diamond lattice by substituting two cabon atoms by a silicon atom and a nearby empty lattice site respectively. The silicon atom occupies its energetically optimal position by sitting in-between two lattice sites. This is called “split-

vacancy" configuration and induces a D_{3d} symmetry with the two vacancies and the impurity alligned along the $\langle 111 \rangle$ diamond axis [**?**], see Figure 2.3.

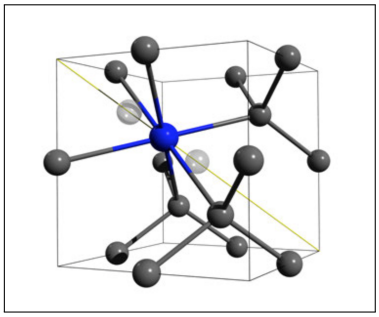

Figure 2.3: Crystal structure of the SiV center embedded into the diamond lattice: The silicon atom (blue sphere) sits in between two vacant lattice sites (white spheres) forming a "split-vacancy" configuration aligned along the $\langle 111 \rangle$ crystallographic axis (yellow line). Figure reproduced with permission from [**?**].

The SiV center is known to occur in two different charge states. The first is the neutral state or SiV^0 with a zero-phonon transition at 1.31 eV (946 nm). It is assoctiated with a $S = 1$ ground state [**?**]. The second state is the negatively charged state SiV^- where the silicon-vacancy center recruited an additional free electron. It exhibits a zero-phonon transition at 1.68 eV (738 nm. Its ground state has been determined as a $S = \frac{1}{2}$ state [**?**, **?**]. Due to its outstanding brightness and the location of the zero-phonon-line in the visible range of the spectrum, this thesis focuses on the negatively charged SiV center. For convenience we drop the charge distinction from now on and refer to SiV^- centers simply as SiV centers.

SiV centers have been created using CVD in nanodiamonds and single-crystal diamond films [**?**], see **??** for details. It is also possible to directly implant silicon atoms into pure diamond. High temperature annealing must then be used to animate present lattice vacancies to recombine with silicon impurities in order to forme split-vacancy SiV centers [**?**, **?**].

In the following sections we detail the most important luminescence properties of SiV centers in diamond. For a comprehensive review we refer to [**?**, **?**] and references therein.

2.3.1 Luminescence properties

The silicon-vacancy center as a quasi-atomic system is capable of absorbing and emmitting light. When a ground state electron absorbs a photon of appropriate energy, it is promoted to a discrete higher-energy excited state located within the band gap of the diamond host matrix. Reversing this excitation relaxes the electron back down to the ground state while emmitting a so-called flourescent photon, accounting for the energy difference between excited and ground state. This transition is "spin-allowed", limiting the life-times of excited states to nano-seconds and thus promoting rapid relaxation and associated fluorescence [**?**].

Since flourescence is directly linked to the electronic structure of the SiV center, see Figure 2.4. It follows that photoluminescence spectroscopy can be used to study it using a laser to optically excite the SiV center. In the context of this thesis, optical above-resonant excitation is the method of choice, in particular, when used in conjunction with a confocal photoluminescence setup which will be discussed in **??**. If the excitation energy exceeds the energy of the

lowest excited state, electrons are promoted to higher electronic and vibrational states. Conveniently, these states relax rapidly towards the lowest exited state in non-radiative processes [?]. Once the lowest excited state is reached, a flouresent transition can follow. It has been shown that above-resonant excitation is feasible for excitation energies ranging from 1.75 eV to 2.55 eV [?, ?, ?]. If the excitation energy is choosen too high, however, the SiV center is ionized. Electrons donated to the diamond conduction band do not participate in flourescence. Ionization may be reversed if a positively charged SiV center manages to capture a free electron from the conduction band. This charge state conversion is believed to be linked to flourencense intermittence, more intuitively named as blinking SiV centers [?, ?].

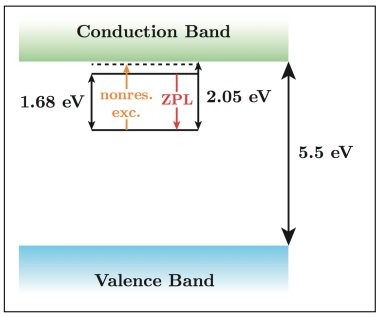

Figure 2.4: Simplified picture of the generous 5.5 eV band gap of diamond with discrete states induced by the presence of SiV centers. The SiV center ground state is situated 2.05 eV below the diamond conduction band. The lowest excited state sits 1.68 eV above the ground state with the zero-phonon-line transition in red connecting the two. Above-resonant optical excitation is indicated in orange. Figure curtesy of [?].

The flourescence spectrum of SiV centers have two prominent features: A narrow zero-phonon-line a broad phonon side band. The former is connected to flourescent photons associated with a purely electronic transition while the latter involves vibrational transitions involving electron-phonon interactions. The phonon side band is typically shifted to higher wavelengths with respect to the zero-phonon-line. The resulting energy deficit can be explained by phonons being created during the relaxation of higher vibrational states. A shift in the opposite direction can also be observed in rare cases if phonons are absorbed during the relaxation process [?].

The relative strength of the zero-phonon-line and the phonon side band is connected to the electron-phonon coupling of the excited color center and thus to lattice vibrations. When a color center is excited, its charge distribution changes. As a result, the equilibrium positions of all particles involved in the color center shift leading to changes in color center geometry. Naturally, the combined changes of charge distribution and geometry of the color center affect the sourrounding atoms of the host lattice. Similarily, if the exited state relaxes back to the ground state, the process occurs in reverse. Thus, due to differing atomic arrangements for ground and exited states, the emmission and absorption of photons is accompanied by lattice vibrations, i.e. phonons. In other words, the electron-phonon interaction couples the motion of the lattice and electronic transitions of a color center [?, ?].

The Huang-Rhys model allows us to discuss the electron-phonon interaction in SiV centers in more detail. Our discussion follows the presentation in [?]. The model assumes in its simplest form that vibrational modes can be modelled as oscillations of nuclei between their euqilibrium coordinates q associated with the electronic states [?]. Let $\mathcal{K}_{^3A_2}(q)$ and $\mathcal{K}_{^3E}(q)$

denote the harmonic potentials of the ground and excited states respectively:

$$\mathcal{K}_{^3A_2}(q) = \frac{1}{2}\Omega^2 q^2 \tag{2.1}$$

$$\mathcal{K}_{^3E}(q) = C_{^3E} + aq + \frac{1}{2}(\Omega^2 + b)q^2 \tag{2.2}$$

$$= C_{^3E} - C_R + \frac{1}{2}(\Omega^2 + b)(q - \delta q)^2. \tag{2.3}$$

It follows that the vibrational modes of ground and exited states are given as harmonic states with disrete energies $\hbar\Omega(\nu + 2)$ as well as $\hbar\sqrt{\Omega + b}(\nu + 2)$ respectively, where ν denotes the occupation number and Ω the frequency. Further, let aq denote the linear nuclear displacement of the excited state configuration with respect to the ground state equilibrium where $q = 0$ holds. The quadratic term bq^2 refers to the vibrational frequency shift due to a redistribution of charge between the electronic states. Given the linear and quadratic electron-phonon coupling strenghts a and b, the equilibrium displacement of the ^3E state can be obtained as:

$$\delta q = \frac{-a}{\Omega^2 + b}, \tag{2.4}$$

while the relaxation energy reads [**?**]:

$$C_R = \frac{a^2}{2(\Omega^2 + b)} = \hbar S\sqrt{\Omega + b}, \tag{2.5}$$

where S is referred to as Huang-Rhys factor.

To reason about the probabilities of various transitions between different vibrational levels associated with ground and excited states, the Franck-Condon principle can be applied [**?**, **?**]. It states that transitions between electronic states become more probable if origin and destination states have vibrational levels with similar energy. This implies that the most probable transitiosn occur between states requiring no change of nuclei positions. Figure 2.5 illustrates the application of the principle for the Huang-Rhys model.

We find that the most probable optical relaxation from an ^3E excited state back to an $^3A_2$ ground state originates from the fundamental vibrational ^3E state, i.e. the lowest-energy excited state. This state is shifted by δq with respect to the ground state, indicating that the energetically optimal nuclei positions differ from their ground state equilibirum positions. The most probable destination of the relaxation is a higher vibrational level of the $^3A_2$ ground state with similar nuclei positions. From there, electron-phonon interactions continue the relaxation process down to the fundamental vibrational level of the ground state. This non-radiative process allows nuclei to return to their original ground staet equilibrium positions. The process of exciting the system from the ground state, proceeds in reverse. The most probable optical excitation promotes an electron from the fundamental $^3A_2$ ground state to a higher vibrational level of the ^3E excited state. The optical transition is such that nuclei positions do not change. Note that optical transitions are faster than vibrational transitions since they do not require a change in nuclei positions. Once in the higher vibrational excited state, electron-phonon interactions mediate a transition down to the fundamental ^3E excited

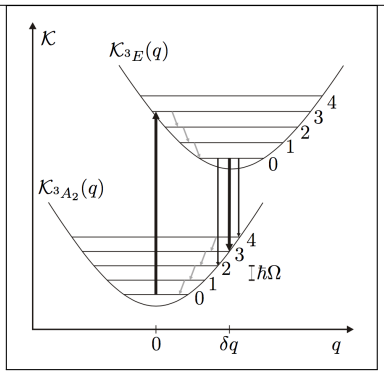

Figure 2.5: Huang-Rhys model of the vibrational transitions in the Frank-Condon picture: The excited state $\mathcal{K}_{^3E}(q)$ is shifted by δq with respect to the ground state potential $\mathcal{K}_{^3A_2}(q)$. The recombination originating at δq marks the most probable transition (thick black arrow) from the fundamental ^3E vibrational level to one of the vibrational levels of the $^3A_2$ ground state followed by non-radiative transitions to the equilibrium position $q = 0$. The number of vibrational quanta involved in an optical transition are determined by the Huang-Rhys factor S. The excitation reverses the process. Optical transitions occur between states with identical values of q and are shown as vertical black arrows. Non-radiative transitions change the value of q and are shown as angled gray arrows. Figure and caption reproduced with permission [**?**].

state with an associated change in nuclei positions. From there the relaxation-excitation cycle and its induced periodic changes in nuclei positions repeats.

As discussed, transitions involving phonons mostly originate from the fundamental vibrational level of excited electronic states and end in higher vibrational states of the electronic ground state. Photons emitted during the relaxation process are associated with the phonon side band of the SiV center. The observed red-shift of the phonon side band is directly tied to the phonon energy with higher order sidebands showing multiples of this energy. Note that the The Huang-Rhys factor S can be interpreted as an indicator of the most probable optical transition involving photons. Thus, it can be used to quantify the strenght of the electron-phonon interactions in SiV centers. A small value of S indicates a weak electron-phonon coupling resulting in neglible phonon side band emmisions. If no phonons are involved, the entire emission is concentrated in the zero-phonon-line. Conversely, a large value of S indicates extensive electron-phonon interactions, leading to a pronounced phonon side band and a weaker zero-phonon-line. This dependence is naturally described by

$$\frac{I_{ZPL}}{I_ZPL + I_PSB} \tag{2.6}$$

For SiV centers hosted in polycrystalline diamonds the Huang-Rhys factors have been determined to be very small ranging from 0.08 to 0.24 [**?**, **?**, **?**]. As a result the zero-phonon-line as the most probable transition dominates the luminescence spectrum making SiV centers excellent narrow-band emitters. Figure 2.6 illustrates the stark difference between the zero-phonon-line and the phonon side band. In contrast, $S = 3.74$ has been established for nitrogen vacancy centers [**?**]. A electron-phonon coupling of this magnitude concentrates almost all emission into the phonon side band and leaves the zero-phonon-line almost indetectable.

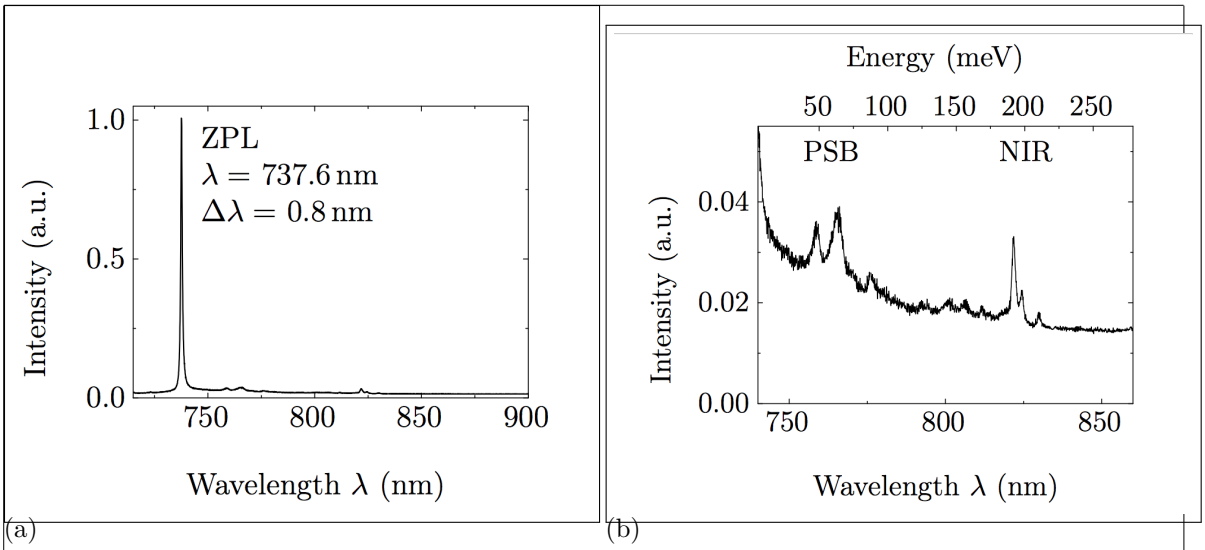

Figure 2.6: (a) The narrow zero-phonon-line dominates the luminescence spectrum. (b) Low intensity phonon side band shows distinct vibrational transitions. Figure reproduced with permission [?].

As an alternative measure for the electron-phonon coupling the Debeye-Waller factor can be used. It is closely reltated to the Huang-Rhys factor and definded as

$$D_w = e^{-S}, \tag{2.7}$$

which can be interpreted as the fraction of total photons that are emitted into the zero-phonon-line.

We remark at this point, that our discussion based on the Huang-Rhys model is assumes that only one vibrational mode couples to the color center which is a strong assumption. In general it is believed that in a solid state host matrix a discrimination between the modes of the undisturbed lattice and quasi-local impurity-induced modes is appropriate [?, ?, ?]. Furthermore, various mechanical properties such as stress in the lattice are reported to affect phonon energies [?]. In addition electron-phonon interactions and thus phonon side band features are believed to depend strongly on various local properties of color centers [?, ?]. Thus it is possible to encounter varying phonon side band features from one SiV center to the next. For a more detailed discussion of these effects we refer the reader to [?, ?] and references therein.

We close this chapter with a short discussion of the luminescence spectra of SiV centers at cryogenic temperatures. Naturally as temperatures approach absolute-zero the phonon side band must disappear. If SiV centers are cooled below $\approx 110\,\mathrm{K}$ a fine structure is revealed [?]. It includes up to 12 different lines with intensities proportional to the natural abundance of the three stable isotopes of silicon $^{28}Si, ^{29}Si, ^{30}Si$ [?]. Each isotope is associated with 4 lines attributed to doublet levels of ground and excited states which are split by 0.2 meV and 1.07 meV respectively [?, ?, ?]. The splitting itself is believed to be a result of spin-orbit coupling with a weak contribution of the dynamic Jahn-Teller effect [?]. Initial results were based on ensembles of SiV centers, however, recently the splitting was detected for isolated

SiV centers as well [?]. Figure 2.7 shows exemplary spectra representative for ensembles and single SiV center at cryogenic temperatures.

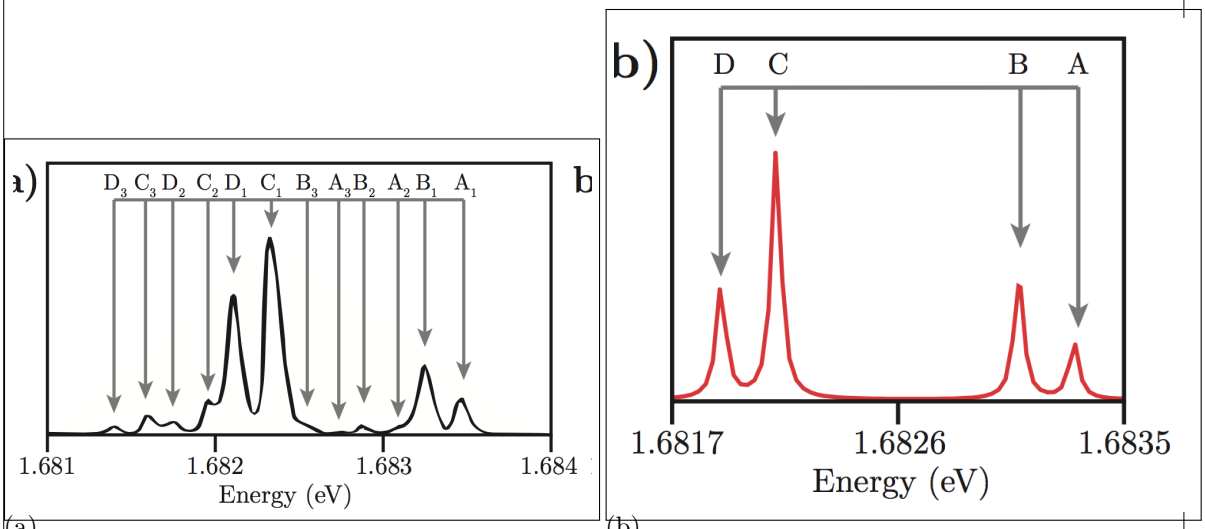

(a) (b)

Figure 2.7: (a) Flourescence spectrum of an enseble of SiV centers at 10 K. 12 peaks can be seen, 4 for each stable isotope of silicon [?]. (b) Flourescence spectrum of an isolated SiV center at 15 K. 4 peaks can be seen, 2 for the ground state and 2 for the excited state. Figure reproduced from [?].